Near Resonantly Enhanced Schlieren
for Wake Flow Visualisation in Shock Tunnels

R. Hruschka, S. O'Byrne and H. Kleine [1]

[1]Department of Aerospace, Civil and Mechanical Engineering
University of NewSouth Wales, Australian Defence Force Academy
Canberra, 2600, AUSTRALIA

Abstract

A new variant of the resonantly enhanced schlieren or shadowgraph technique has been developed for visualising flows with small density gradients using seeded lithium metal as the resonant species. The novelty of the technique lies in the use of a diode laser as the light source for the visualisation rather than systems based upon solid-state-pumped dye lasers or spectral lamps. We present time-resolved visualisations of near-wake flows around a cylinder in a hypersonic freestream in a shock tunnel, showing flow structures that cannot be resolved using a conventional standard schlieren system. Furthermore, a method of removing, at least partially, the limitation related to line-of-sight visualisation is demonstrated.

Introduction

Schlieren and shadowgraph techniques are mature methods for visualising flows in transparent fluid media containing density gradients. While they are simple and nonintrusive, these techniques can become ineffective at showing more subtle flow features that are not associated with strong density gradients. In gaseous media where the refractive index is close to unity, $\partial n/\partial y \approx \partial \rho/\partial y$. Thus the contrast on an image can be determined by the relation [9]

$$\frac{I}{I_0} = \frac{f_2}{na} \int_{\xi_1}^{\xi_2} \frac{\partial n}{\partial y} dz. \qquad (1)$$

By changing the optical and geometrical properties of the system, i.e. the second lens focal length f_2 or the unobstructed source image height a, the contrast and thus the sensitivity can be increased. This can be done, however, only to a limited extent. The practical limit is reached when natural density fluctuations in the ambient laboratory atmosphere add too much background noise to the image, overwhelming the desired features of flow visualisation. One other method for enhancing the sensitivity of density-sensitive techniques involves increasing the refractive index n using the enhanced refractivity $(n-1)$ near resonant transitions of atoms or molecules, which are either an intrinsic component of the flow or seeded into it. In the absence of Doppler-broadening, the frequency-dependent refractive index in gaseous media can be described by the following equation:

$$n = 1 + \frac{N_i q_e^2}{2 m_e \varepsilon_0} \sum_i \frac{(\omega_{0i}^2 - \omega^2) f_i}{(\omega_{0i}^2 - \omega^2)^2 + \gamma_i^2 \omega^2} \qquad (2)$$

Multiple transitions with center frequency ω_{0i}, damping constants γ_i and oscillator strengths f_i contribute to the total refractive index. In case of air, the refractivity slowly increases towards the blue with a peak in the vacuum UV. The concept of resonant refractivity, however, is based on a sharp increase close to a much stronger single transition. As the achievable resonant amplification is approximately proportional to $1/(\omega_{0i} - \omega)$ as well as f_i, a narrowband light source tuned slightly off a ground state transition will provide the best results. Atomic transitions are strongly in favour of molecular transitions due to their much higher f_i values and ground state populations N_i. The Li D2 line used in our work is therefore effectively more than five orders of magnitude stronger than any molecular transition of either N_2, O_2, or NO, which naturally occur in our hypersonic freestream. The behaviour of refraction and absorption in the vicinity of the Li D1/D2 doublet at 1500 K and a pressure of 0.01 atm, which are typical values for our flowfield, is shown in figure 1. Heat transfer calculations show that the seeding ratio of 0.5 % is readily achieved if lithium metal is deposited in the nozzle reservoir of our shock tube. The refractive index curve is based on equation 2, although Doppler broadening is considered by inserting the Doppler-shifted frequency $\omega_D = \omega_0(1 + v/c)$ for ω and integrating over a two-dimensional Maxwell-Boltzmann velocity distribution. In practice, a diode-laser based system tuned to the refractivity peak is not feasible due to the high absorption rates close to the line center. However, further off resonance the ratio of absorption to refraction drops off by approximately $1/\omega$. At several tens of picometers (pm) detuning, the medium will be transparent enough to enable diode lasers to be used for high-speed schlieren applications.
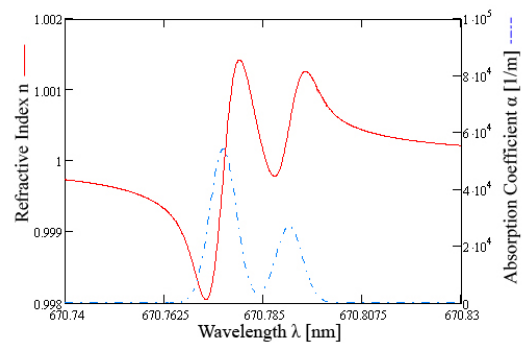

Figure 1: Refractive index and absorption coefficient: Li D2(670.776 nm) and Li D1(670.791 nm) transitions.

Previous enhanced refractivity experiments

In several experiments the refractivity in rarefied flows was increased by orders of magnitude taking advantage of resonant refractivity. Light sources composed of spark gaps or flash lights combined with interference filters are usually fairly broadband spectral light sources compared to lasers. However, in earlier years, they have been successfully used to achieve resonant enhancement of refractivity of more than two orders of magnitude (Leonard *et al.* [6]), enough to visualise wake structures of supersonic projectiles in atmospheres of less than one per cent of ambient density. Whereas incoherent light sources usually provide a higher dynamic range of schlieren systems and noise-

free images, higher sensitivities are achieved with lasers due to their high intensity, narrow line shape and spatial accuracy. The combination of sodium as a seeding species and a pulsed dye laser was used for near-resonant shadowgraphy of flows around toroidal aerocapture ballutes at the GALCIT T5 shock tunnel facility by Rasheed *et al.* [11]. The sodium was introduced by spraying a solution containing NaCl on the shock tube end wall. McIntyre *et al.* [8] showed that the possibilities applying interferometry to hypersonic flows can be vastly extended by resonant enhancement. Bishop *et al.* [1] have demonstrated that even with only small seeding ratios of sodium the technique is much more effective than attempting to take advantage of molecular transitions. If the refractivity-enhancing species is introduced only locally into the flow, selected flow features can be visualised separately. Lemieux *et al.* [5] attached small lumps of sodium to a wire stretched across the flowfield upstream of a cone of the T5 facility. The streaklines caused by the evaporating sodium were successfully used to analyse boundary layer structures. As in this approach local absorption was more desired than local refraction, the dye laser used was tuned exactly to the D2 line.

Our Experiments at T-ADFA

T-ADFA is a free piston driven shock tunnel. The conical nozzle with 300 mm exit diameter creates a diverging Mach 10 flow of N_2 at two different conditions, which are described in table 1. The Reynolds number (*Re* #) is based on the model diameter. A 400 mm long cylinder with 32 mm diameter was used as a model. This is much wider then the core flow of about 200 mm diameter. For this reason, another wire-mounted cylinder only 140 mm long was used in some experiments in order to check for effects caused by the nozzle boundary layer.

Condition		A	B
Enthalpy	H_o [MJ/kg]	13.5	4.0
Reservoir Pressure	P_{res} [MPa]	12	12
Reservoir Temperature	T_{res} [K]	7200	3100
Freestream Pressure	P_∞ [KPa]	0.36	0.25
Freestream Temperature	T_∞ [K]	568	142
Freestream Density	ρ_∞ [kg/m^3]	0.002	0.006
Freestream Velocity	u_∞ [m/s]	4560	2510
Freestream Re #	Re	1.0×10^4	4.7×10^4

Table 1: Flow conditions for tunnel experiments.

Choice of Seed Species

Alkali metals are particularly suitable due to their strong $n_s - n_p$ transitions in the visible or near IR. Other experimenters almost exclusively used NaCl or Na as a resonant species. We preferred Li, as it is the least reactive of all alkali metals, and reactions with shock tunnel components can be neglected. Furthermore formation of molecules containing Li is suppressed by the high temperatures in the nozzle reservoir. The Li was introduced in the form of a metal foil of graduated thickness into the nozzle reservoir of our T-ADFA shock tunnel facility. This strategy overcomes the only disadvantage of Li, namely its higher boiling point (1615 K) compared to other alkali metals (< 1160 K) and also ensures that the seeding is homogeneous enough for the flow time of interest. The Li D1 (670.791 nm) and D2 lines (670.776 nm) are so closely spaced that in practice both lines will enhance refractivity for detunings > 10 pm. Due to its low mass, the predominantly Doppler broadened absorption/refraction profiles of Li are 1.5-3 times wider than lines of other alkali metals, and therefore allow the refractivity to be more precisely chosen. The comparatively high ionisation potential also favours Li to Na, K, Rb or Cs, as most atoms can be

expected to be in the electronic ground state. Furthermore, Li is the only element with D lines in the visible region where diode lasers are commercially available.

Suitable Light Sources

In order to get a high refractivity, the overlap integral of the refractivity curve and light source spectral distribution should be as large as possible. However, as the refractivity drops off more slowly than the absorption curve, large refractions combined with low absorption can be realised when the light source peaks somewhere in the wings of the absorption line. Spectral narrowness is desired to a certain degree, but is not as crucial as it is for other spectroscopic applications like absorption spectroscopy. With the high seeding ratios in our experiments, even a light source with a FWHM of several hundred pm provides good results - a fact most welcome, as most high-powered diode lasers operate multimode with linewidths in this range. It should be mentioned that cancellations of refractions in opposite directions might occur if the absorption line center is within the emission profile of the light source. These cancellations can be avoided if a schlieren system sensitive to refractions in any arbitrary direction is used. However, if it is desired to choose a specific value of refractivity, a narrowband, single mode diode laser has to be used. Single-longitudinal-mode diode lasers like the 10-mW Hitachi HL6714G used in our work are narrowband but with low output power, which turned out to be problematic for some of our experiments. Also, random frequency instabilities (mode-hops), which are typical for single mode Fabry-Perot laser diodes, introduce a random element into the experiments.

Optics and Imaging Systems

A lens based schlieren system [9] was used for the experiments, with a 0.25-m focal-length collimating lens and a 1-m focal-length focussing lens. Longer focal lengths and mirrors were initially used, but illumination was not adequate using the 10-mW diode. Even this optically fairly insensitive system was able to capture weak density fluctuations in the wake that were totally invisible in the absence of seeding. Our resonantly enhanced flow visualisation system was developed in order to analyse the wake flow starting process behind a cylinder and to determine the flow steadiness. For time-resolved imaging, a Shimadzu Hypervision HPV-1 high-speed camera operating with frame rates up to 1000 kfps was used. However, the 125 kfps setting was found to be the best compromise between sufficient frame illumination and temporal resolution.

Effects of Resonant Enhancement

Figure 2 shows the effect of resonant enhancement at the low density of condition A. In the absence of Li seeding, only the bow shock can be visualised. The wake shows no flow features at all (a). The black lines are parts of the mounting system which has been changed in the course of the experimental campaign. With Li in the flow and the diode laser tuned 55 pm downwards from D2, the average calculated refractivity is about 370 times higher than the value for air, and thus all important wake flow features like lip shocks, recompression shocks, and expansion fans are clearly resolved (b). However, the disadvantages of the technique can be also observed: The exposure is rather dark due to the calculated average absorption rate of approximately 0.4/m.

Another side effect of the Li seeding becomes obvious when figure 2 (a) is compared with figure 2 (b). The flow luminosity in the stagnation region of the cylinder is significantly increased. Flow luminosity is caused by collisional electronic excitation and successive radiative decay. Its intensity depends on the excited state population and the radiative decay rate. At 6500 K,
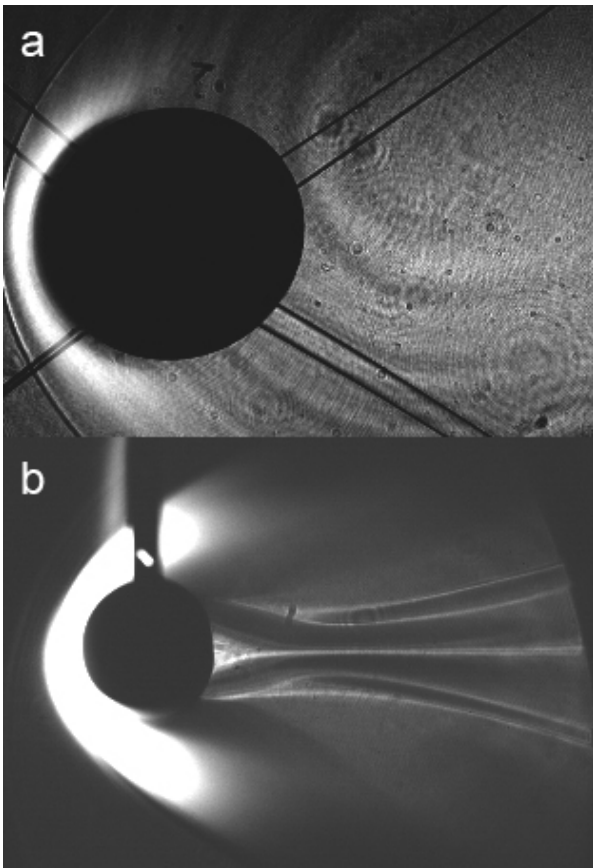
Figure 2: Conventional (A) and resonantly enhanced (B) schlieren of a hypersonic flow around a cylinder (condition A, see table 1). Images are reproduced in different scales.

the Li 2_p state will have an equilibrium population of about 0.4 %, compared to 0.0015 % of the N_2 molecules in their first excited ($A^3\Sigma_u^+$) state. Furthermore the radiative lifetime of Li 2_p is only 27 ns, so most of the transitions will be radiative. The N_2 ($A^3\Sigma_u^+ \longrightarrow X^1\Sigma_g^+$) transition on the other hand is forbidden, leading to most of the transitions being non-radiative. Thus a Li seeding of 0.5 % leads to a considerably higher luminosity behind the bow shock compared to non-seeded conditions. However, as the average temperature of the wake region is much lower, no luminosity is created there and thus the main area of interest is not affected by luminosity.

Local Refractivity Enhancement

Near-resonance-enhanced schlieren offers the possibility to only visualise the flow in selected planes. In some of these experiments the seeding material is introduced locally, by depositing a small piece of lithium foil onto the middle of the model forebody. The high stagnation-point temperatures cause the Li to evaporate, leading to near-resonant refractivity enhancement in a slice of the base region no wider than 10 mm. Because in this experiment a high absorption coefficient does not affect the overall picture brightness, the laser was tuned to a wavelength only 25 pm downwards from D2. This resulted in a calculated refractivity increase of about 700, compared to the value for air. A comparison of the slice with flow features integrated along the line of sight at condition A is shown in figure 3. All characteristic features of the base flow are visible in both slice (a) and line-of-sight (b) picture. The model surface is marked as a circle. The symmetry line is marked as a line. The charac-

teristic lip shock (1), the shear layer (2), the slipstream (3) and the recompression shock (4) are nearly at the same locations for both experiments, indicating that the nozzle boundary layer and the flow divergence do not significantly compromise the assumption of quasi-two-dimensional flow. A feature of nearly all exposures taken is the dark region between outer edge of slip stream (3) and recompression shock (4), indicating an overranged schlieren system and thus a fairly high density gradient. By reducing the sensitivity it was found that the outer edge of this dark region represents the recompression shock.
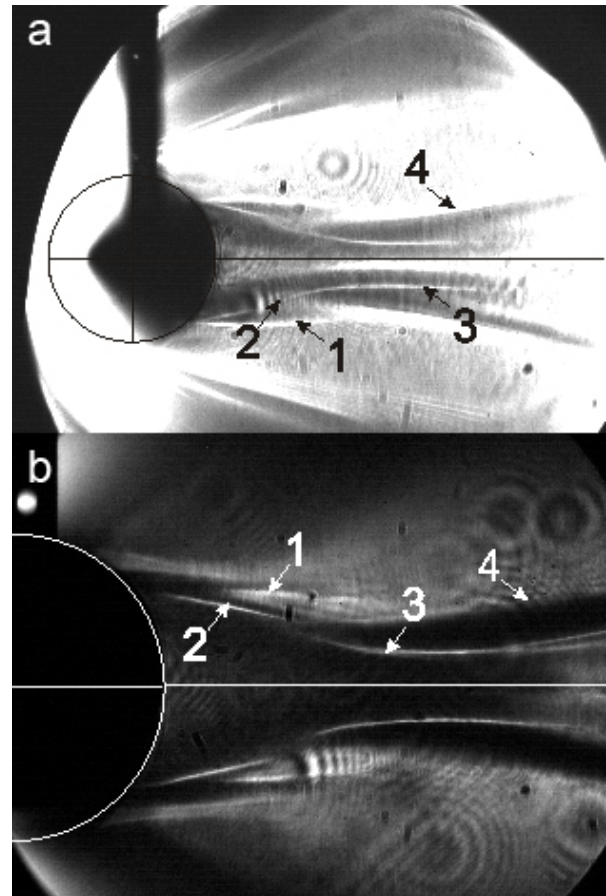

Figure 3: Enhanced schlieren - locally introduced at the front of the cylinder (a) and globally introduced in the nozzle reservoir (b). The model dimensions and the symmetry line are marked. Images are reproduced in different scales.

Steady Flow Features

Characteristic for hypersonic flows is a strong lip shock caused by overexpansion of the detached shear layer shortly after separation. The lip shock in figures 3(a+b) originates slightly downstream of and below the separation point, which is consistent with Hama's findings [3], although our Mach numbers are two times as high. Hama also found that for laminar flow, the separation angle increases with decreasing Reynolds number. This tendency was also observed in our experiments, as the Reynolds number at condition B is 4.7 times higher than at condition A. He also reports a tendency that for high Mach and Reynolds numbers, lip shock (1) and recompression shock (4) tend to become inseparable, without crossing each other. While for low Mach numbers combined with high Re the lip shock is a straight line, an outwards curvature is typical for high Mach/low Re numbers [3]. These tendencies can be observed particularly in figure 2(b).

The flow separation point from the cylinder could be clearly determined in most of the pictures taken. The detachment angle could be measured for both conditions. At condition A, the flow separates at 136 (+/-3) degrees, which is consistent with data found in the literature [7] [2]. For higher Reynolds numbers (condition B) the flow separation angle was found to be 127 (+/-3) degrees. The separation angles measured from the schlieren images coincide with minima of heat transfer measurements on a cylinder model with the same diameter and a length of 132 mm at the same facility [10]. The divergence angle of the recompression shock was found to be 7.5 (+/-1) degrees at condition A and 11.5 (+/-1) degrees at condition B. The rear stagnation point was found to be further downstream at condition B compared to condition A. Increasing wake lengths with decreasing Re are general tendencies also found by Larson [4], although the Mach numbers in his experiments were only around Mach three.

Unsteady Wake Startup Process

At condition B the wake needs about 400–500 μs from arrival of the flow to reach a steady state, i.e. a flow pattern with only minor changes over time. This is approximately the same time as the centreline pitot trace takes to reach a constant value. Condition B has been chosen because of a longer flow time with constant freestream pressure compared to condition A. The startup process is shown in figure 4. Figure 4 (a) shows the situation 100 μs after flow arrival, when the N_2-Li mixture is engulfing the model. The strong flow features like the far-wake structures become visible first. Figure 4 (b) shows the gas entrainment into the base region with the establishment of the near-wake eddies 120 μs later. The freestream pressure continues to rise, so that the formed eddies acquire more angular momentum from the free shear layer, causing them to become more circular, as shown in figure 4 (c). Figure 4 (d) shows the situation about 290 μs after flow arrival. At this stage, the central reverse flow has enough momentum to separate the eddies and drive them off the centreline. The reverse flow region in between appears detached in the center. Between 300 and 400 μs after flow arrival, the freestream pressure drops to its steady value. This enables the gas entrained in the eddies to mix with the free shear layer and escape through the wake neck (e). 490 μs after flow arrival, a steady flow is established (f). No inner wake structures are visible in picture f, which is probably due to a lack of Li in the recirculation region. However, other experiments indicated that the eddies will come close to the centerline again, indicating less momentum of the central flow at steady state.

Conclusions

A diode-laser based schlieren system for high-speed flow imaging has been introduced. The effect of resonant refractivity on sensitivity was demonstrated. A calculated sensitivity increase of up to 700 compared to a non-resonant system allowed weak wake structures to be visualised. The limitation of line-of-sight techniques has been reduced by seeding a particular region of the flow. The transient startup process of a wake flow around a cylinder has been presented as a possible application. However, the weak light source in combination with high absorption rates was detrimental to the picture quality.

Acknowledgements

References

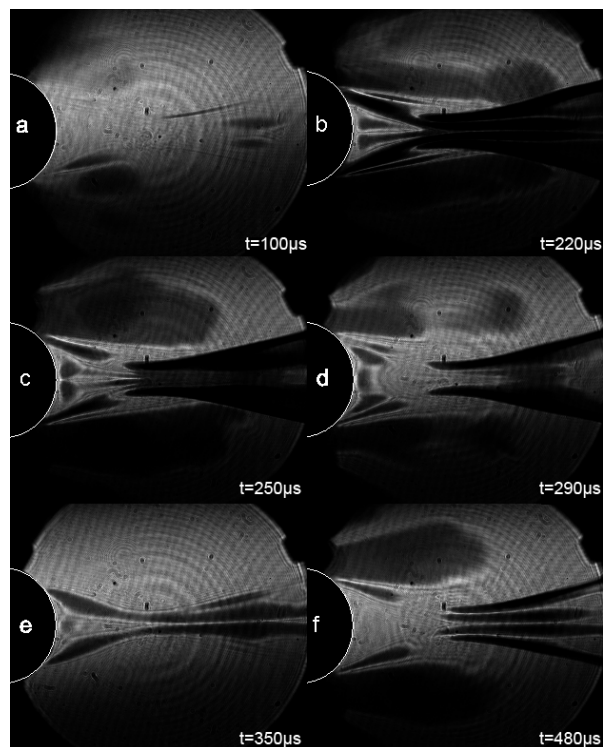[1] Bishop, A., *Spectrally Selective Holographic Interferome-*

Figure 4: Flow starting process around a cylinder at condition B (a-f). The numbers indicate the time after flow arrival (μs). The model dimensions are marked with a white line.

try Techniques for Flow Diagnostics, Ph.D. thesis, Department of Mechanical Engineering, University of Queensland, 2001.

[2] Gregorek, G. M. and Korkan, K. D., An experimental observation of the Mach and Reynolds number independence of cylinders in hypersonic flow, *AIAA Journal*, **1**, 1963, 210–211.

[3] Hama, R., Experimental investigations of wedge base pressure and lip shock, Technical Report 32-1033, NASA Jet Propulsion Laboratory, 1966.

[4] Larson, R., Scott, C., Elgin, D. and Selver, R., Turbulent base flow investigations at Mach Number 3, Technical Report N64-15888, University of Minnesota, Institute of Technology, Rosemont Aeronautical Laboratories, Rosemont, Minnesota, 1962.

[5] Lemieux, P. and Hornung, H. G., Development and application of streakline visualisation in hypersonic flows, *Experiments in Fluids*, **33**, 2002, 188–195.

[6] Leonard, D. A. and Keck, J. C., Schlieren photography of projectile wakes using resonance radiation, Technical report, AVCO Everett, 1962.

[7] McCarthy Jr., J. F. and Kubota, T., A study of wakes behind a circular cylinder at m=5.7, *AIAA Journal*, **2**, 1964, 629–636.

[8] McIntyre, T., Bishop, A., Eichmann, T. and Rubinsztein-Dunlop, H., Enhanced flow visualisation with near-resonant holographic interferometry, *Applied Optics*, **42**, 2003, 4445–4451.

[9] Merzkirch, W., *Flow Visualization*, Academic Press, 1987, 2 edition.

[10] Park, G., Gai, S. L., Neely, A. J. and Hruschka, R., Base pressure and heat transfer on planetary entry type configurations, in *Proceedings of the 26th International Symposium on Shock Waves*, 2007.

[11] Rasheed, A., Fujii, K., Hornung, H. and Hall, J., Experimental investigation of the flow over a toroidal aerocapture ballute, in *AIAA Paper 2001-2460*, 2001.